

Short communication

Preparation of alumina/carbon nanotubes composites
by chemical precipitationQi Yang, Yida Deng, Wenbin Hu^{*}*State Key Laboratory of Metal Matrix Composites, Shanghai Jiaotong University, 800 Dongchuan Road, Shanghai 200240, China*

Received 3 December 2007; received in revised form 15 April 2008; accepted 28 May 2008

Available online 19 July 2008

Abstract

Continuous alumina coating on multi-walled carbon nanotubes (MWCNTs) was successfully prepared by a new method of chemical precipitation using aluminum nitrate and ammonia as starting materials. Structure and morphology of the alumina/multi-walled carbon nanotubes ($\text{Al}_2\text{O}_3/\text{MWCNTs}$) composites were characterized by transmission electron microscopy (TEM), high resolution transmission electron microscopy (HRTEM), energy-dispersive X-ray spectroscopy (EDX), X-ray diffraction (XRD), infrared spectra (IR), thermo gravimetric analysis (TG), differential thermal analysis (DTA) and N_2 adsorption–desorption. The results show that polyvinyl alcohol (PVA) modification on the surface of MWCNTs contributes to form continuous alumina coating, $\gamma\text{-Al}_2\text{O}_3$ layers with thickness of 1–3 nm cover the surface of MWCNTs and the original structure of MWCNTs is retained during the coating process.

© 2008 Elsevier Ltd and Techna Group S.r.l. All rights reserved.

Keywords: B. Composites; Alumina; Carbon nanotubes; Coating; Chemical precipitation**1. Introduction**

Since the discovery of carbon nanotubes (CNTs), they have been receiving much attention over the past decade because of their properties such as small dimension, big area, high strength, unique conductivity and applications in reinforce of composites, field emission devices, chemical sensors and nano-electrical devices [1–5]. CNTs can substitute carbon fibers as reinforcements in composites because of their tremendous properties. However, before CNTs are used as reinforcing additives in composites, there are two major obstacles such as the dispersibility of CNTs in matrix and undesirable interface reaction between CNTs and matrix at high temperature [6,7]. Coating technology on the surface of CNTs was the most efficient method to overcome these problems and improve the mechanical properties at the same time, such as alumina coating, titania coating, and etc. [8].

Presently, various methods have been reported to load CNTs with functional nanoparticles, such as decorating MWCNTs with iron oxide nanoparticles using a chemistry precipitation

method [9], Pt nanoparticles using supercritical carbon dioxide deposition [10], Cu and Ni using electroless plating method [11], ceria nanoparticles by supercritical hydrothermal synthesis method [12], anatase TiO_2 nanoparticles by sol–gel and rutile TiO_2 nanorods by hydrothermal methods [13].

However, there are few reports about the synthesis of alumina/multi-walled carbon nanotubes ($\text{Al}_2\text{O}_3/\text{MWCNTs}$) composites [14–16]. Li et al. immersed MWCNTs into aluminum nitrate solution, then calcinated under N_2 atmosphere at 500 °C to synthesize $\text{Al}_2\text{O}_3/\text{MWCNTs}$ composites with sponge-like morphology, and their adsorbility of fluorination in water was studied [14]. MWCNTs decorated with alumina nanoparticles were prepared by an impregnation method using aluminum isopropoxide (AIP) as inorganic sources and decomposed by hydrolysis on the surface of carbon nanotubes [15]. Lee et al. filled and coated MWCNTs with alumina by chemical vapor deposition [16].

In this paper, in order to provide a favourable dispersibility and prevent harmful interface reaction for CNTs in matrix, we propose a simple chemical precipitation to synthesize continuous alumina coating on the surface of MWCNTs modified by PVA. The chemical precipitation process, the effects of PVA and the characterization of composites were discussed.

^{*} Corresponding author. Tel.: +86 21 34202554; fax: +86 21 62822012.

E-mail address: wbh@263.net (W. Hu).

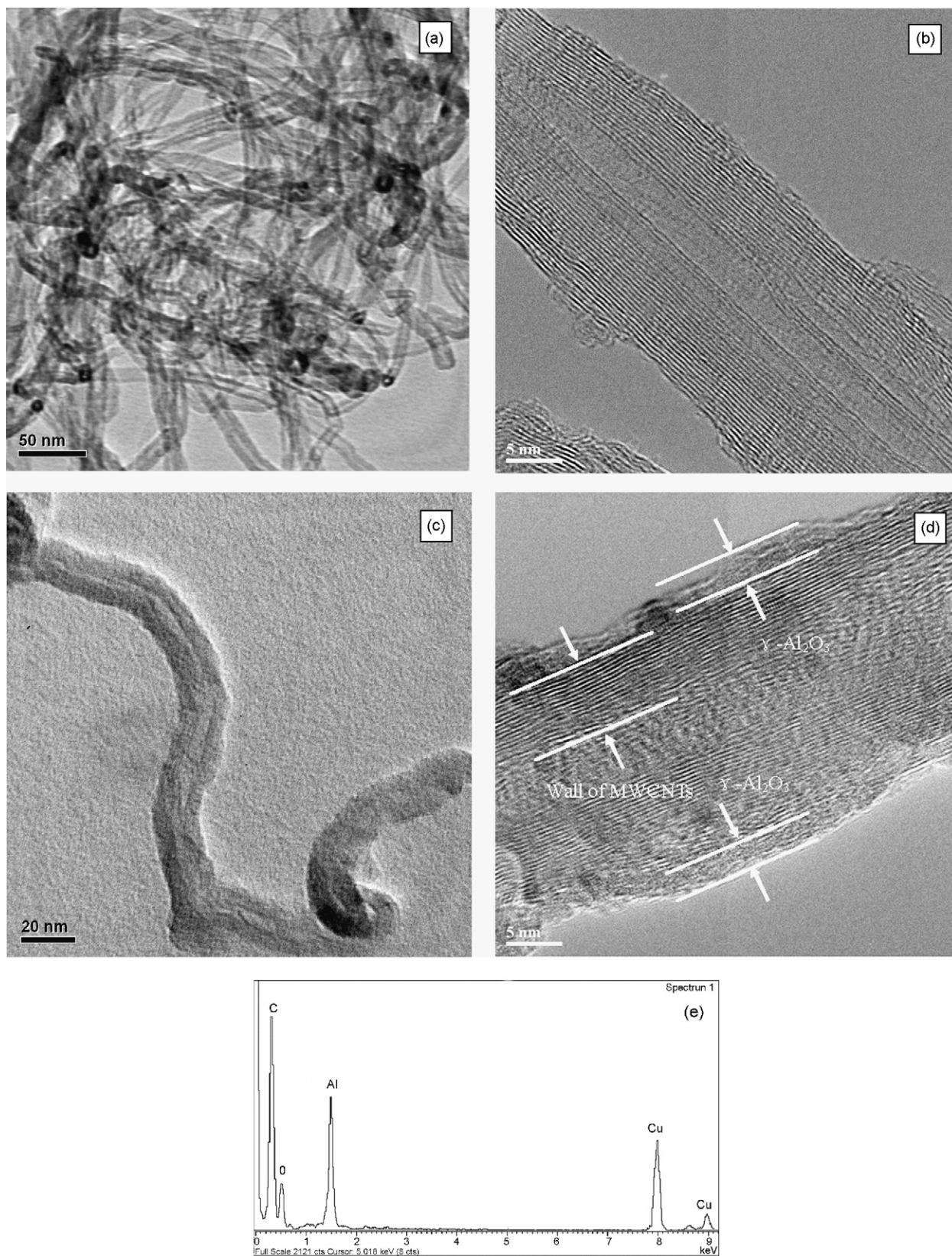


Fig. 1. TEM images of pristine MWCNTs (a), alumina/MWCNTs composites (c) and HRTEM images of MWCNTs (b), alumina/MWCNTs composites (d), and EDX spectrum of composites (e).

2. Experimental

MWCNTs with purity of 95% were provided by Shenzhen Nanotech Port Co., Ltd., which were prepared by the catalytic decomposition of CH_4 using La_2NiO_4 as catalyst precursor. To remove the catalyst, MWCNTs were purified via being dispersed in a 1 M HNO_3 solution for more than 6 h, followed by filtering and washing with distilled water several times. PVA with polymerization degree of 1750 is commercially pure. $\text{Al}(\text{NO}_3)_3 \cdot 9\text{H}_2\text{O}$, $\text{NH}_3 \cdot \text{H}_2\text{O}$, HNO_3 , H_2SO_4 are analytic pure. All the reagents were used without further purification. A typical preparation procedure of $\text{Al}_2\text{O}_3/\text{MWCNTs}$ composites was as follows: To modify the surface of MWCNTs, 1.0 g of purified MWCNTs was dispersed in a 100 ml PVA aqueous solution (2.5 wt%) for 6 h, then the suspension was filtered, washed with distilled water several times to remove the residual PVA, and dried at 60°C in vacuum for 12 h. Subsequently, 0.5 g PVA-modified MWCNTs was dispersed into 100 ml $\text{Al}(\text{NO}_3)_3$ (10 wt%) solution by ultrasonic treatment. Then the ammonia solution with a concentration of 2.5 wt% was added dropwise into the suspension with vigorously agitation until the pH value reached 9.5. After agitated for 1 h, the insoluble black products were filtered, washed with distilled water and dried at 60°C in vacuum for 12 h. Finally, the precipitated products were heated in N_2 atmosphere from room temperature too 500°C at the heat rate of $3^\circ\text{C}/\text{min}$ and kept for 2 h, and about 0.6 g $\text{Al}_2\text{O}_3/\text{MWCNTs}$ composites were obtained.

The morphology and chemical component of the products were examined by means of transmission electron microscopy (TEM), high resolution transmission electron microscopy (HRTEM) and energy-dispersive X-ray spectroscopy (EDX) on a JEOL JEM-2010 equipped with an energy-dispersive X-ray spectrometer, employing an accelerating voltage of 200 kV. X-ray diffraction (XRD) was recorded on a BRUKER-AXS X-ray powder diffractometer with $\text{Cu K}\alpha$ radiation ($\lambda = 0.154178 \text{ nm}$) in the range of $10^\circ < 2\theta < 80^\circ$ at a scanning speed of $1^\circ/\text{min}$. The infrared absorption spectra (IR) was measured on an EQUINOX55 Fourier transform infrared spectroscope using KBr pellets from 400 to 4000 cm^{-1} at a resolution of 2 cm^{-1} . The zeta potential was measured with a Zetaplus analyzer (Zetasizer 2000). Each sample was ultrasonicated for 1 h prior to analysis. The ionic strength was maintained at 10^{-3} M using NaCl . TG and DTA were performed on a TG 2050 thermo gravimetric analysis (TG) from room temperature to 800°C and a DTA 1600 differential thermal analysis (DTA) from room temperature to 1000°C at a heating rate of $10^\circ\text{C}/\text{min}$ in air. The N_2 absorption–desorption isotherms at liquid nitrogen temperature (78 K) were measured by ASAP2010 static volumetric absorption analyzer. BET surface area was calculated based on the adsorption data in the relative pressure range of $p/p_0 = 0.05\text{--}0.25$.

3. Results and discussion

Fig. 1a shows the TEM image of pristine MWCNTs. The pristine MWCNTs are curved and twisted with each other. Their length is several micrometers and the average external

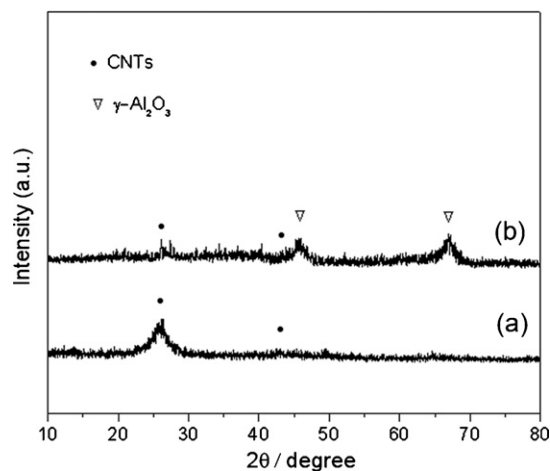


Fig. 2. XRD patterns of (a) pristine MWCNTs and (b) alumina/MWCNTs composites.

diameter is about 10–30 nm. HRTEM image of the MWCNTs indicates that their carbon atoms arrange orderly and their tubular structure is very clear (Fig. 1b). Fig. 1c represents the rough and compact surface of the $\text{Al}_2\text{O}_3/\text{MWCNTs}$ composites, compared with the MWCNTs. It seems that the surface of nanotubes has been coated with some products, which are testified as $\gamma\text{-Al}_2\text{O}_3$ in the XRD analysis (Fig. 2b). Fig. 1d shows a representative HRTEM image of the $\text{Al}_2\text{O}_3/\text{MWCNTs}$ composites, illustrates clearly the periodic multiwalls of the MWCNTs and the $\gamma\text{-Al}_2\text{O}_3$ coating layers, and the thicknesses of the $\gamma\text{-Al}_2\text{O}_3$ layers are about 1–3 nm. Fig. 1e displays the EDX spectrum taken from the $\text{Al}_2\text{O}_3/\text{MWCNTs}$ composites in Fig. 1d. Only the C-, O-, Al-related peaks are present in the EDX spectrum, revealing that the covered products is indeed Al_2O_3 ; the Cu-related peaks in the spectrum come from the Cu grids.

Fig. 2 displays the XRD patterns of pristine MWCNTs and $\text{Al}_2\text{O}_3/\text{MWCNTs}$ composites. The two peaks at 26.02° and 42.68° correspond to (0 0 2) and (1 0 1) reflections of MWCNTs, respectively (Fig. 2a) [17]. From Fig. 2b, the two peaks of MWCNTs are much lower than that of pure MWCNTs, and the two peaks at 45.86° and 67.03° are

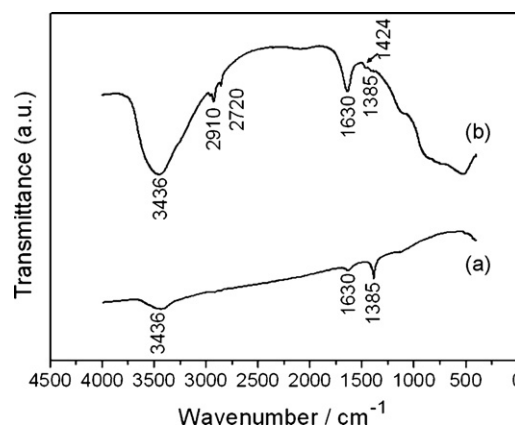


Fig. 3. IR patterns of (a) pristine MWCNTs and (b) alumina/MWCNTs composites.

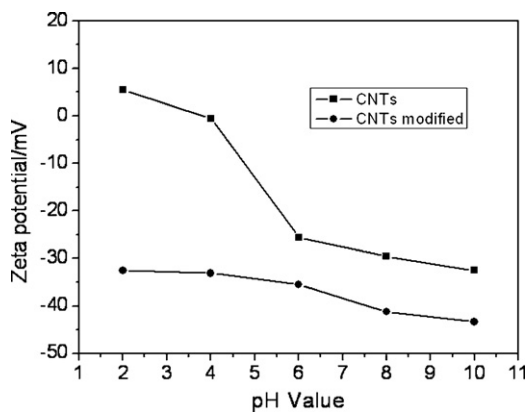


Fig. 4. Zeta potentials of pristine MWCNTs and MWCNTs modified by PVA.

assigned to (4 0 0) and (4 4 0) reflections of γ - Al_2O_3 (JCPDS Card 10-0425). Therefore, the composites should be considered as nanosized MWCNTs coated by γ - Al_2O_3 .

IR spectra are helpful to further understand the formation of Al_2O_3 /MWCNTs composites. The IR spectra of pristine MWCNTs are shown in Fig. 3a. The band at 1385 cm^{-1} is assigned to the C–C vibration, the band at 3436 and 1630 cm^{-1} are assigned to the O–H stretch and bend vibration of adsorbed water. In Fig. 3b, compared with pure MWCNTs (Fig. 3a), the very broad and smooth band from 400 to 1000 cm^{-1} demonstrate the feature of nano-alumina [18]. The band at 1424 , 2720 and 2910 cm^{-1} correspond to the C–H stretch and bend vibration, originated from the surface of MWCNTs modified by PVA [19,20].

Fig. 4 shows zeta potential of pristine MWCNTs and MWCNTs modified by PVA. When the pH value of solution is above 4, the MWCNTs are negatively charged. The modification of MWCNTs by PVA further decreases the zeta potential value of all pH values studied. It means that the modification of MWCNTs by PVA can generate more functional groups on the surface graphite layers of MWCNTs.

Based on above analysis, a simulation scheme is proposed to illustrate the whole process for the preparation of Al_2O_3 /MWCNTs composite (Fig. 5). After MWCNTs modified by PVA, the hydrophobic groups (–OH) of PVA incorporate with MWCNTs by Van Der Waals force, their hydrophilic groups extend into solution, and induce MWCNTs become more negative. Al^{3+} ions incorporate with hydrophilic group (–OH) by electrostatic force [21]. After aqueous ammonia was added dropwise into solution, Al^{3+} ions change to alumina hydrate

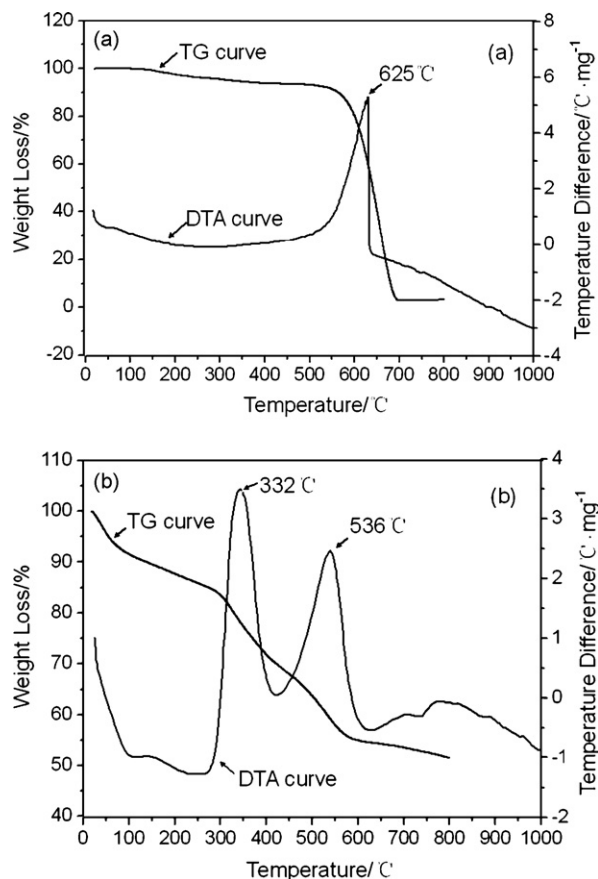


Fig. 6. TG and DTA curves of (a) pristine MWCNTs and (b) the precipitated products.

which deposits on the surface of MWCNTs and transforms to γ - Al_2O_3 after calcinated at $500\text{ }^\circ\text{C}$ for 2 h.

The heat treatment process of pristine MWCNTs and the precipitated products was analyzed by TG and DTA. According to the DTA curve of Fig. 6a, the exothermic peak around $625\text{ }^\circ\text{C}$ can be assigned to the ignition of MWCNTs and there is a corresponding 98% weight loss in the TG curve (Fig. 6a). The ignition residues are chiefly ferric oxide and silicate, which are introduced in the growth process. On the other hand, there are visible differences in the composites (Fig. 6b). First, the total weight loss is about 46%, less than that of the MWCNTs. Second, there are two exothermic peaks at 332 and $536\text{ }^\circ\text{C}$, the exothermic peaks at $332\text{ }^\circ\text{C}$ correspond to the ignition of PVA [22], and the exothermic peaks at $536\text{ }^\circ\text{C}$ correspond to the

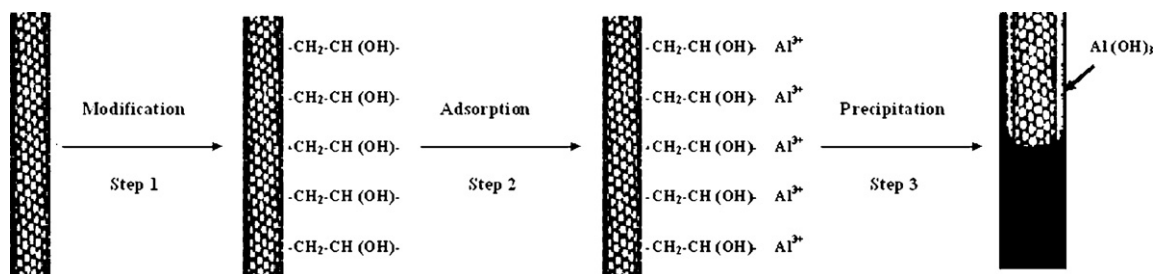


Fig. 5. Schematic representation of synthesis of alumina/MWCNTs composites.

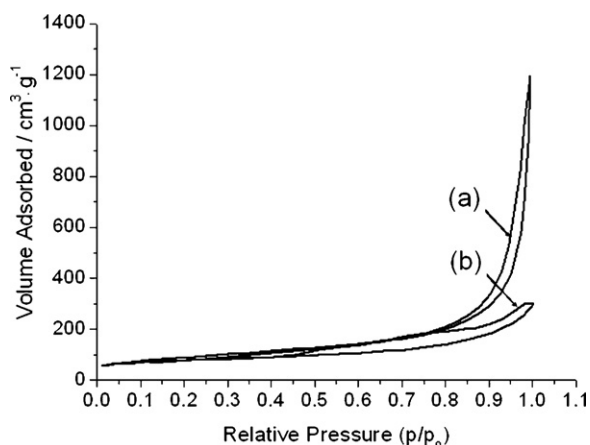


Fig. 7. Adsorption-desorption isotherms of (a) pristine MWCNTs and (b) alumina/MWCNTs composites.

Table 1
Nitrogen adsorption-desorption analysis data of MWCNTs and composites

Samples	Carbon nanotubes	Composites
BET surface area ($\text{m}^2 \text{g}^{-1}$)	314.03	168.39
Pore volume ($\text{cm}^3 \text{g}^{-1}$)	1.85	0.42
Pore diameter (nm)	9.1	5.5

ignition of MWCNTs, which is much lower than that of pure MWCNTs. Finally, the broad endothermic scale from 220 to 270 °C is observed, which contribute to the decomposition of $\text{Al}(\text{OH})_3$.

The nitrogen adsorption and desorption isotherms of pristine MWCNTs and $\text{Al}_2\text{O}_3/\text{MWCNTs}$ composites are presented in Fig. 7. The isotherm of MWCNTs is type IV (BDDT classification) and has type H3 hysteresis loops, associated with aggregates of platelike particles giving rise to slit-like pores [23]. The isotherm of the composites is type IV and has two types of hysteresis loops. At low relative pressure $0.45 < p/p_0 < 0.85$, the hysteresis loop is type H2, which can be observed in the pores with narrow necks and wider bodies (ink-bottle pores) [23], perhaps because the Al_2O_3 block the pores of MWCNTs, when they deposit on the surface of MWCNTs. At high relative pressure between $0.85 < p/p_0 < 1$, the shape of the hysteresis loops is type H3. BET surface area, pore volume and pore diameter of MWCNTs and composites are listed in Table 1. After MWCNTs coated with Al_2O_3 , the BET surface area, pore volume and pore diameter of MWCNTs significantly reduced from 314.03 to 168.39 $\text{cm}^2 \text{g}^{-1}$, 1.85 to 0.42 $\text{cm}^3 \text{g}^{-1}$, 9.1 to 5.5 nm, respectively. This directly proved that Al_2O_3 cover the surface of the MWCNTs and block their pores.

4. Conclusions

The $\text{Al}_2\text{O}_3/\text{MWCNTs}$ composites with continuous alumina coatings on the surface of MWCNTs were fabricated by chemical precipitation. During the process, PVA-modified MWCNTs and contributed to form the continuous alumina

coatings. The alumina coating was $\gamma\text{-Al}_2\text{O}_3$, and their thickness is about 1–3 nm.

Acknowledgments

This work was supported by the National Science Foundation of China (Grant No. 50401004). We thank Analysing Center of Shanghai Jiaotong University for the characterization of TEM and XRD.

References

- [1] S. Iijima, Helical microtubules of graphitic carbon, *Nature* 354 (1991) 56–58.
- [2] P. Calvert, Strength in disunity, *Nature* 357 (1992) 365–366.
- [3] W.A.D. Heer, A. Châtelain, D. Ugarte, A carbon nanotube field-emission electron source, *Science* 270 (1995) 1179–1181.
- [4] J. Kong, N.R. Franklin, C. Zhou, M.G. Chapline, S. Peng, K. Cho, H. Dai, Nanotube molecular wires as chemical sensors, *Science* 287 (2000) 622–625.
- [5] H. Dai, J.H. Hafner, A.G. Rinzler, D.T. Colbert, R.E. Smalley, Nanotubes as nanoprobe in scanning probe microscopy, *Nature* 384 (1996) 147–150.
- [6] E.W. Wong, P.E. Sheehan, C.M. Lieber, Nanobeam mechanics: elasticity, strength and toughness of nanorods and nanotubes, *Science* 277 (1997) 1971–1975.
- [7] J.P. Salvetat, G.D. Briggs, J.M. Bonard, R.R. Bacsá, A.J. Kulik, N.A. Burnham, L. Forró, Elastic and shear moduli of single-walled carbon nanotube ropes, *Phys. Rev. Lett.* 82 (1999) 944–947.
- [8] K. Hernadi, E. Ljubovic, J.W. Seo, L. Forró, Synthesis of MWNT-based composite materials with inorganic coating, *Acta Mater.* 51 (5) (2003) 1447–1452.
- [9] H.Q. Cao, M.F. Zhu, Y.G. Li, Decoration of carbon nanotubes with iron oxide, *J. Solid State Chem.* 179 (2006) 1208–1213.
- [10] A. Bayrakceken, U. Kitkamthorn, M. Aindow, C. Erkey, Decoration of multi-wall carbon nanotubes with platinum nanoparticles using supercritical deposition with thermodynamic control of metal loading, *Scripta Mater.* 56 (2007) 101–103.
- [11] L.M. Ang, T.S.A. Hor, G.Q. Xu, C.H. Tung, S.P. Zhao, J.L.S. Wang, Decoration of activated carbon nanotubes with copper and nickel, *Carbon* 38 (2000) 363–372.
- [12] D. Zhao, E. Han, X. Wu, H. Guan, Hydrothermal synthesis of ceria nanoparticles supported on carbon nanotubes in supercritical water, *Mater. Lett.* 60 (2006) 3544–3547.
- [13] X.H. Xia, Z.J. Jia, Y. Yu, Y. Liang, Z. Wang, L.L. Ma, Preparation of multi-walled carbon nanotube supported TiO_2 and its photocatalytic activity in the reduction of CO_2 with H_2O , *Carbon* 45 (2007) 717–721.
- [14] Y.H. Li, S.G. Wang, A.Y. Cao, D. Zhao, X.F. Zhang, C.L. Xu, Z.K. Luan, D.B. Ruan, J. Liang, D.H. Wu, B.Q. Wei, Adsorption of fluoride from water by amorphous alumina supported on carbon nanotubes, *Chem. Phys. Lett.* 350 (2001) 412–416.
- [15] K. Hernadi, E. Ljubović, J.W. Seo, L. Forró, Synthesis of MWNT-based composite materials with inorganic coating, *Acta Mater.* 51 (2003) 1447–1452.
- [16] J.S. Lee, B. Min, K. Cho, S. Kim, J. Park, Y.T. Lee, N.S. Kim, M.S. Lee, S.O. Park, J.T. Moon, Al_2O_3 nanotubes and nanorods fabricated by coating and filling of carbon nanotubes with atomic-layer deposition, *J. Cryst. Growth* 254 (2003) 443–448.
- [17] Y.H. Li, J. Ding, J.F. Chen, C.L. Xu, B.Q. Wei, J. Liang, D.H. Wu, Preparation of ceria nanoparticles supported on carbon nanotubes, *Mater. Res. Bull.* 37 (2) (2002) 313–318.
- [18] C.H. Shek, J.K.L. Lai, T.S. Gu, G.M. Lin, Transformation evolution and infrared absorption spectra of amorphous and crystalline nano- Al_2O_3 powders, *Nanostruct. Mater.* 8 (1997) 605–610.
- [19] A. Tawansi, A. El-Khodary, M.M. Abdelnaby, A study of the physical properties of FeCl_3 filled PVA, *Curr. Appl. Phys.* 5 (2005) 572–578.

- [20] Y. Badr, M.A. Mahmoud, Effect of PVA surrounding medium on ZnSe nanoparticles: size, optical, and electrical properties, *Spectrochim. Acta A* 65 (2006) 584–590.
- [21] H. Rafati, E.C. Lavelle, A.G.A. Coombes, S. Stolnik, J. Holland, S.S. Davis, The immune response to a model antigen associated with PLG microparticles prepared using different surfactants, *Vaccine* 15 (17–18) (1997) 1888–1897.
- [22] W.P. Yang, S.S. Shyu, E.G. Lee, A.C. Chao, Effects of PVA content and calcination temperature on the properties of PVA/boehmite composite film, *Mater. Chem. Phys.* 45 (2) (1996) 108–113.
- [23] K.S.W. Sing, D.H. Everett, R.A.W. Haul, L. Moscou, R.A. Pierotti, J. Rouquerol, T. Siemieniowska, Commission on colloid and surface chemistry including catalysis, *Pure Appl. Chem.* 57 (1985) 603–619.